

Covalent Immobilization of Aggregation-Induced Emission Luminogens in Silica Nanoparticles Through Click Reaction

Faisal Mahtab, Jacky W. Y. Lam, Yong Yu, Jianzhao Liu, Wangzhang Yuan, Ping Lu, and Ben Zhong Tang*

Fluorescent silica nanoparticles (FSNPs) with efficient light emission, colloidal stability, and size tunability are fabricated by one-pot, two-step Stöber and reverse microemulsion techniques. Tetraphenylethene (TPE)- and silole-functionalized siloxanes are facilely synthesized by click reactions and their sol-gel reactions followed by reactions with tetraethoxysilane generate FSNPs with core-shell structures. The FSNPs are uniformly sized with smooth surfaces, and show high surface charges and hence excellent colloidal stability. UV irradiation of ethanol solutions of the FSNPs gives strong blue and green light at 474 and 486 nm in high fluorescence quantum yields, thanks to the novel aggregation-induced emission attributes of the TPE and silole aggregates in the hybrid nanoparticles. The FSNPs are benign to living cells and function as fluorescent visualizers for intracellular imaging of HeLa cells.

1. Introduction

The fabrication of fluorescent silica nanoparticles (FSNPs) has been a fast-growing research area for the last two decades because of their potential applications in a number of nanotechnological fields ranging from biological to advanced engineering. Much interest has been placed on the construction of FSNPs with controlled size, high monodispersity and fluorescence quantum yield, and good colloidal stability at

physiological pH.^[1] There are numerous features that make silica nanoparticles superior to their polymeric counterparts, such as good hydrophilicity and easy surface modification.^[2–6] They also show high thermal stability and possess a large surface area and excellent dispersion in aqueous media. As silica nanoparticles are nonfluorescent and chemically inert, they are environmentally friendly and are an ideal host material for the inclusion of fluorophores and magnetic clusters.

Both inorganic and organic (fluorescein, rhodamine, etc.) fluorophores are used for the preparation of FSNPs. Among them, semiconductor quantum dots (QDs) have attracted much attention, particularly in the area of cellular marking or imaging, because of their advantages of size-tunable emission color, long luminescence lifetime, and high resistance to photobleaching. Their surface, however, needs to be functionalized in order to improve their hydrophilicity and reduce their toxicity as QDs are usually chalcogenides of heavy metals (e.g., CdSe, ZnSe, CdS, and PdTe), which are well-known toxicants or carcinogens.^[7–11]

FSNPs can be prepared by incorporating fluorophores into the silica networks via physical processes or chemical reactions. The silica matrix acts as a protective shield, which reduces the likelihood of penetration of oxygen and other harmful species that may cause photobleaching of the embedded fluorophores.^[12–14] FSNPs synthesized by the

Dr. F. Mahtab, Dr. J. W. Y. Lam, Y. Yu, Dr. J. Liu, Dr. W. Yuan, Dr. P. Lu, Prof. B. Z. Tang

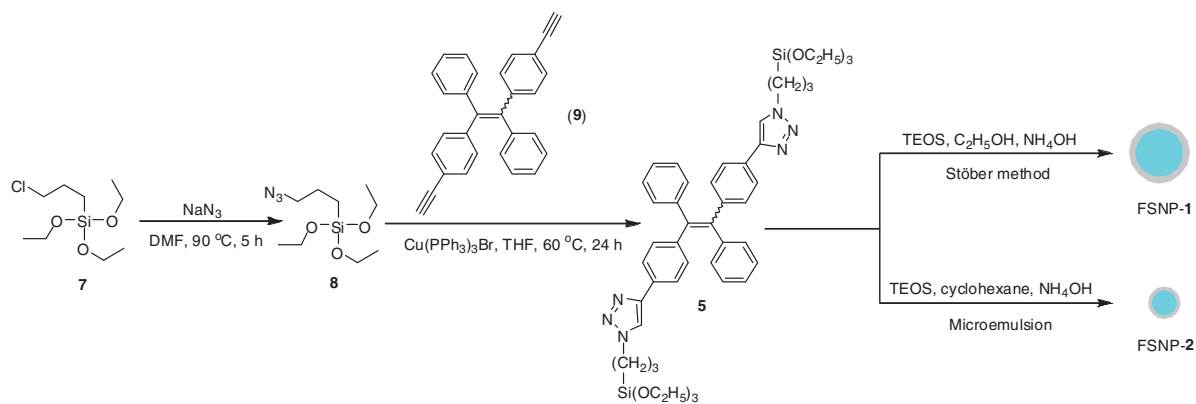
Department of Chemistry
The Hong Kong University of Science & Technology (HKUST)
Clear Water Bay, Kowloon, Hong Kong
E-mail: tangbenz@ust.hk

Dr. F. Mahtab, Dr. J. W. Y. Lam, Y. Yu, Dr. J. Liu, Dr. W. Yuan, Dr. P. Lu,

Prof. B. Z. Tang
HKUST Fok Ying Tung Research Institute
Nansha, Guangzhou, China

Prof. B. Z. Tang
Department of Polymer Science and Engineering
Zhejiang University
Hangzhou 310027, China

DOI: 10.1002/sml.201002195



Scheme 1. Fabrication of TPE-containing fluorescent silica nanoparticles FSNP-1 and FSNP-2.

Stöber method suffer from size limitation to below 100 nm. To overcome this problem, reverse microemulsion has recently gained tremendous attention for the fabrication of nanosized, monodispersed FSNPs.

Development of fluorescent bioprobes with high signal changes in the presence of analytes is a hot research topic. However, light emissions from most of the FSNPs prepared so far using conventional organic dyes have been rather weak. This is due to the emission quenching caused by the aggregation of the fluorophores in the solid state.^[15] A low fluorophore loading in the nanoparticle may be free of aggregation but can offer only a weak fluorescence signal. The light emission can be further weakened, rather than enhanced, if more fluorophores are loaded into the nanoparticles, because of the notorious aggregation-caused quenching (ACQ) effect.^[16]

We have discovered an “abnormal” phenomenon of aggregation-induced emission (AIE) that is exactly opposite to the ACQ effect: a group of propeller-like, nonemissive molecules is induced to emit efficiently by aggregate formation.^[17–21] The AIE effect greatly boosts the emission efficiency of the luminogens, and turns them from weak luminophores into strong emitters. An example is represented by 4,4′-bis(1,2,2-triphenylvinyl)biphenyl, of which the quantum yields in the solution ($\Phi_{F,S}$) and aggregate ($\Phi_{F,A}$) states are ≈ 0 and 100%, respectively, which results in an infinitely large AIE effect ($\alpha_{AIE} = \Phi_{F,A}/\Phi_{F,S} \rightarrow \infty$).^[17] Mechanistic investigations reveal that the AIE effect is caused by the restriction of the intramolecular rotations of the luminogens in the aggregate state, which block the nonradiative channels and populate the radiative decay.^[22–25]

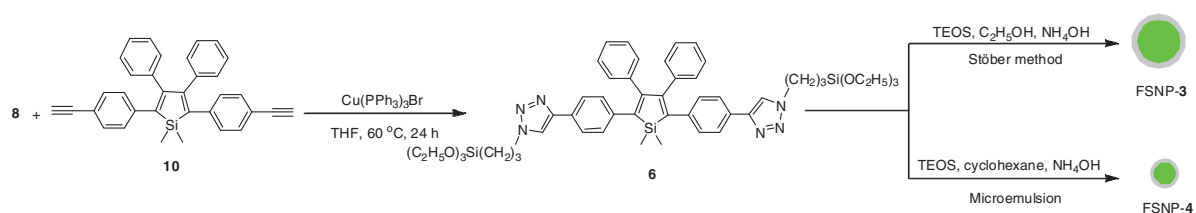
1,3-Dipolar cycloaddition was discovered by Huisgen in 1984.^[26] Later, Sharpless and co-workers found that this reaction can be accelerated by Cu(I) species. They coined it as

a “click” reaction due to its high efficiency and selectivity, mild reaction conditions, and simple isolation procedure.^[27] Organic fluorophores have been incorporated chemically into the silica matrix through an ester or thiourea linkage, which makes them not leak out from the FSNPs under harsh conditions.^[28–30] Few papers have, however, reported the utilization of click chemistry to covalently link fluorophores to silica nanoparticles. In this work, we explored the possibility of hybridizing silica nanoparticles with AIE luminogens by click chemistry. We have developed a facile one-pot, two-step protocol for their preparation. The resultant FSNPs are monodispersed and show high surface charges and hence excellent colloidal stability. Thanks to the AIE effect of the fluorophores and the inert nature of the silica, the FSNPs emit strong visible light upon photoexcitation and function as fluorescent visualizers for intracellular imaging of HeLa cells.

2. Results and Discussion

2.1. Synthesis of FSNPs

To explore the utility of click chemistry for the fabrication of highly emissive FSNPs, we synthesized tetraphenylethene (TPE)- and silole-containing diynes (**9** and **10**, see **Scheme 1** and **2**) according to our previously reported procedures.^[31,32] We also prepared azide-functionalized siloxane **8** in high yield by reaction of 3-chloropropyltriethoxysilane (**7**) with sodium azide in dry dimethylformamide (DMF) at 90 °C for 4 h. To covalently bind the AIE luminogens to the silica nanoparticles at the molecular level, we employed **8** as a chemical linker. We carried out the click reaction of **8** and **9** in the presence of Cu(I) species in distilled tetrahydrofuran



Scheme 2. Synthesis of silole derivative **6** and fabrication of its fluorescent silica nanoparticles FSNP-3 and FSNP-4.

(THF) at 60 °C under nitrogen. The reaction product gives an $(M + 1)^+$ peak at 875.4327 in its high-resolution (HR) mass spectrum (Figure S1 in the Supporting Information, SI), thereby confirming the occurrence of the cycloaddition reaction and the formation of expected adduct **5** ($M^+ = 874.4269$). Employing the same conditions, silole-functionalized siloxane **6** was successfully synthesized from **8** with **10**, as confirmed by the HR mass spectrum given in the SI, Figure S2.

FSNPs with core-shell structures can be prepared from **5** by using the Stöber and reverse microemulsion techniques. In the former method, the molecules of **5** are hydrolyzed and condensed in an ethanol/water mixture containing ammonium hydroxide under stirring at room temperature for 30 min. The resultant TPE-silica nanocores are then subjected to further sol-gel reaction with tetraethoxysilane (TEOS) to furnish FSNP-1 (Scheme 1). Microemulsion is a well-known method to produce nanometer-sized particles with narrow distribution. The formation of a thermodynamically stable nanoreactor is facilitated by the introduction of Triton-X as amphiphilic surfactant. A hydrophilic head region is formed with numerous nanometer-sized water cores and each with a hydrophobic tail that extends into an apolar continuous phase of cyclohexane. The nanodroplets of water in the bulk-oil phase act as nanoreactor for discrete particle formation. After addition of adduct **5**, the mixture was stirred at room temperature for 30 min. The synthesized TPE-silica nanocores then undergo further sol-gel reaction with TEOS, to generate small-sized FSNP-2 with core-shell architecture.

Similarly, coupling of **8** with **10** affords adduct **6** and its two-step sol-gel reaction in one-pot Stöber and reverse microemulsion protocols produces FSNP-3 and FSNP-4, respectively.

Analysis by zeta potential analyzer at room temperature shows that all the FSNPs are monodispersed with low polydispersities down to 0.005 (Figure 1 and Figure S3). The mean diameters of FSNP-1 and FSNP-3 are 185.7 and 255.6 nm, respectively, which are somewhat larger than those measured by transmission electron microscopy (TEM; 143.37 ± 10.5 and 217.26 ± 20.4 nm for FSNP-1 and FSNP-3, respectively) due to the larger hydrodynamic diameters of the FSNPs in

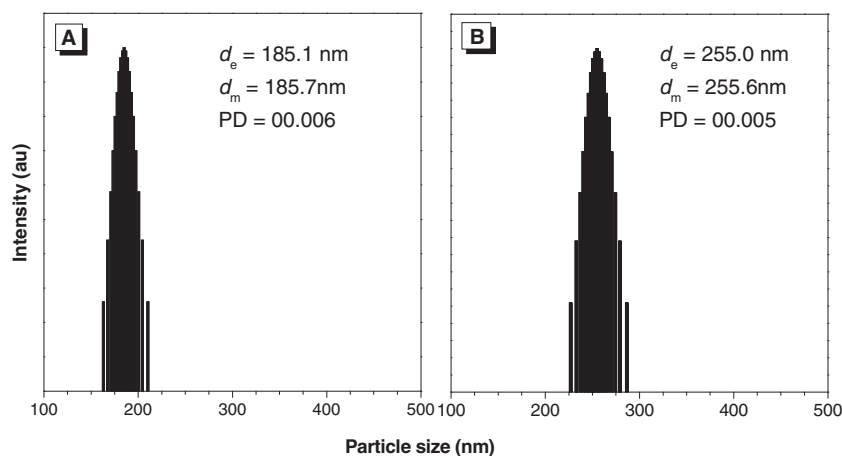


Figure 1. Particle size distributions of A) FSNP-1 and B) FSNP-3. Abbreviations: d_e = effective diameter, d_m = mean diameter, PD = polydispersity.

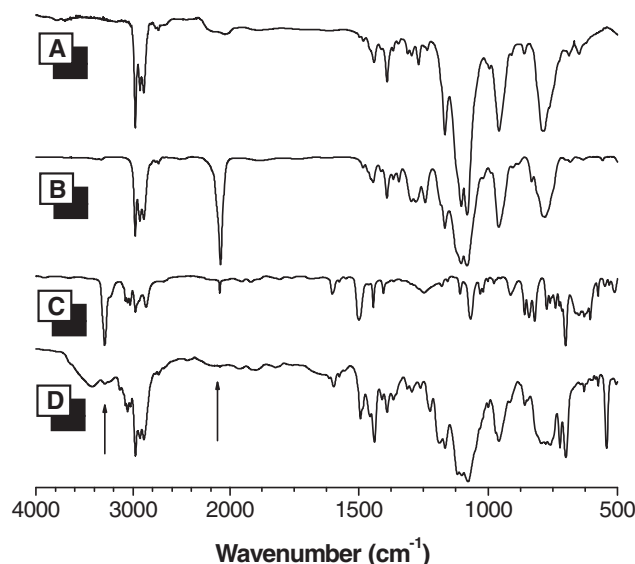


Figure 2. IR spectra of A) **7**, B) **8**, C) **9**, and D) **5**.

the aqueous mixtures and their shrinkages under the high electron-beam intensity in the TEM chamber.

2.2. Structural Characterization

Figure 2 shows the IR spectrum of **5**; for comparison, the spectra of **7–9** are also provided. The azido stretching vibration of **8** is observed at 2098 cm^{-1} , which is absent in **5** (Figure 2D). The spectrum of **5** also shows no peaks associated with the $\text{HC}\equiv$ and $\text{C}\equiv\text{C}$ stretching vibrations of **9** at 3291 and 2107 cm^{-1} . These results suggest that the azido groups of **8** have cyclized with the triple bonds of **9** to form triazole rings in **5**. Similar observations are also found when comparing the spectrum of **6** with those of **8** and **10** (Figure S4).

Analysis by energy-dispersive X-ray (EDX) diffraction of the FSNPs shows that they contain the expected elements of carbon, nitrogen, oxygen, and silicon. Examples of the EDX spectra of FSNP-1 and FSNP-3 are provided in Figure S5, and Table S1 (SI) gives the compositions.

2.3. Size and Morphology

It is important to tune the sizes of nanoparticles to meet the requirements of different technological applications. The Stöber and reverse microemulsion methods give large- and small-sized FSNPs, respectively. Actually, the sizes of the nanoparticles can also be tuned by varying the reaction parameters. Larger nanoparticles are obtained by using higher concentrations of TEOS and ammonium hydroxide and vice versa, as demonstrated by our recent publication.^[33] TEM images show that the large-sized

FSNPs possess smooth surfaces, while the surfaces of the small nanoparticles (i.e., FSNP-2 and FSNP-4) are somewhat rough (**Figure 3** and Figure S6). Analyses by scanning electron microscopy (SEM) also give similar results (**Figure 4** and Figure S7). The mean diameters of FSNP-2 and FSNP-4 determined by TEM are $\approx 37.68 \pm 2.7$ and 59.82 ± 4.1 nm, respectively, thus proving that the reverse microemulsion method does indeed generate FSNPs with much smaller sizes than those prepared by the Stöber technique in a controlled fashion.

2.4. Light Emission

The AIE luminogens are chemically linked to and covered by the inert silica shell, which protects them from direct exposure to the harsh environments as well as their potential leakage to the media. Even if a small amount of the dye molecules is leaked out, it will not interfere as the dissolved fluorophores will not emit (hence no background signals). This is a “bonus” or added advantage of the AIE dyes over their conventional dye counterparts. **Figure 5** shows the fluorescence spectra of **9** and **10** and the suspensions of their core-shell nanoparticles FSNP-1 and FSNP-3 in ethanol. Nearly no fluorescence signals are recorded when the solutions of **9** and **10** are photoexcited, because the multiple phenyl rings of **9** and **10** undergo active intramolecular rotations in the solutions, which effectively annihilate their excited states and hence render them nonemissive.^[27–30] When the molecules of **9** and **10** are covalently incorporated into, and aggregated in, the silica networks, strong fluorescence spectra peaked at 474 and 489 nm are recorded in FSNP-1 and FSNP-3, respectively. The rigid silica networks largely restrict the intramolecular rotations of the luminogens. This blocks the nonradiative relaxation channels and populates the radiative decay, thus making the FSNPs highly luminescent.

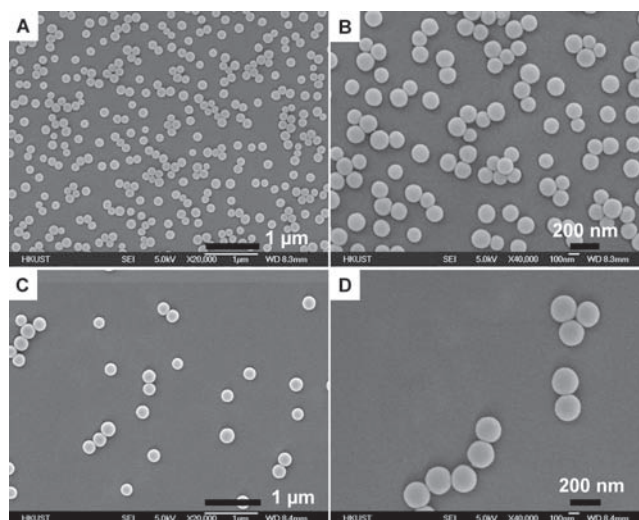


Figure 4. SEM images of A,B) FSNP-1 and C,D) FSNP-3 at different magnifications.

By dissolving **9** and **10** and dispersing FSNP-1 and FSNP-3 fabricated by using the same molar quantities of luminogens (i.e., **5** and **6**) in ethanol, their emission intensities are compared. The light emission from FSNP-1 and FSNP-3 is 1010- and 916-fold higher than those of **9** and **10**, respectively. The absolute fluorescence quantum yields (Φ_{abs}) of FSNP-1 and FSNP-3 determined by integrating spheres are 33.4 and 38.2%, respectively. The light emission is very stable, with no change in the fluorescence spectra detectable after the FSNPs were placed on shelves for several months without protection from light and air. **Figure 6** shows photographs of ethanol solutions of **9** and **10** and the suspensions of FSNP-1 and FSNP-3 taken under UV irradiation. Whereas the solutions of **9** and **10** are nonemissive, intense blue and green light is observed in FSNP-1 and FSNP-3, respectively.

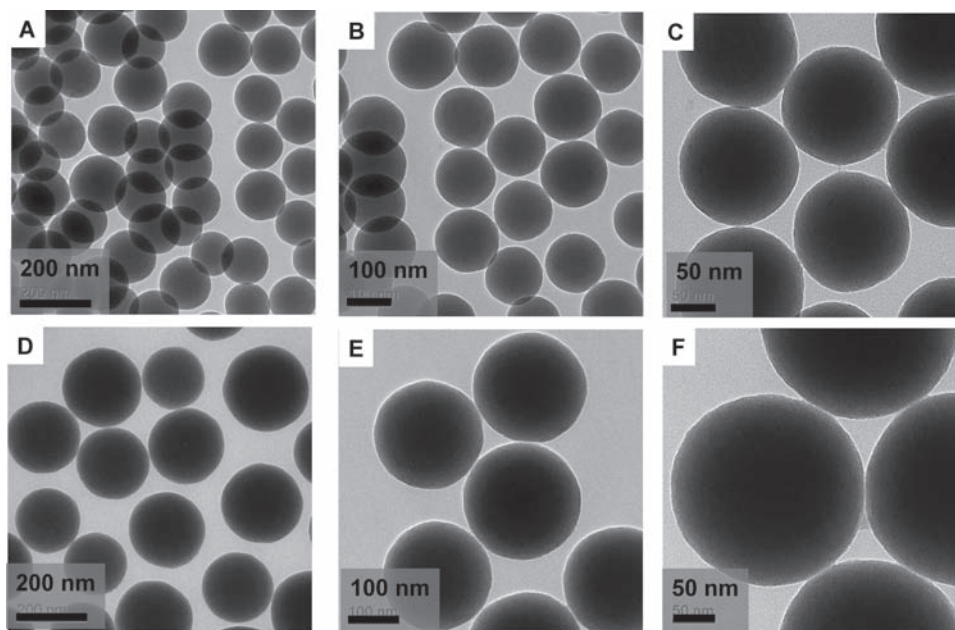


Figure 3. TEM images of A–C) FSNP-1 and D–F) FSNP-3 at different magnifications with particle sizes of $\approx 143.37 \pm 10.5$ and 217.26 ± 20.4 nm, respectively.

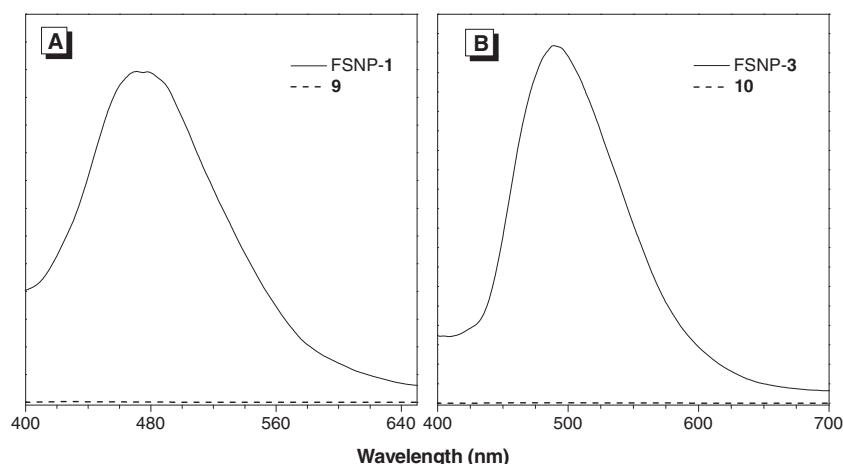


Figure 5. Fluorescence spectra of ethanol solutions of A) FSNP-1 and **9** and B) FSNP-3 and **10**. Concentration: 200 $\mu\text{g mL}^{-1}$; excitation wavelength: A) 353 and B) 370 nm.

The fluorescence spectra of FSNP-2 and FSNP-4 are given in Figure S8 (SI). The emissions of FSNP-2 and FSNP-4 are observed at slightly longer wavelengths than those of FSNP-1 and FSNP-3. Compared with FSNP-1 and FSNP-3, the Φ_{abs} values of FSNP-2 and FSNP-4 are slightly lower (32.8 and 35.0% for FSNP-2 and FSNP-4, respectively), which is understandable when taking into account that the dye loadings used for the construction of FSNP-2 and FSNP-4 are only half of those for FSNP-1 and FSNP-3. Since FSNP-2 and FSNP-4 exhibit much smaller particle sizes, this results in higher dye density and stronger aggregation and thus a red shift in the fluorescence spectra. The photographs shown in **Figure 7** further demonstrate the different emission behaviors between FSNP-1/FSNP-3 and FSNP-2/FSNP-4 pairs. This visual observation also supports the notion that the intramolecular rotations of **5** and **6** are restricted by their covalent incorporation into the silica matrix.

2.5. Colloidal Stability

Colloidal stability is an important parameter for FSNPs and can be reflected by their surface charges or zeta

potentials. FSNPs are said to be colloidally stable if their surface charges are high at the workable pH because strong electrostatic repulsion will exist between the nanoparticles. The functional groups play an important role in determining the surface charges of the FSNPs. In our previous work, we reacted brominated TPE and silole with 3-aminopropyltriethoxysilane (APS) and used the adducts as fluorescent cores for the fabrication of highly emissive and monodispersed FSNPs.^[33] Their charges at neutral pH are, however, not high enough to impart high colloidal stability. This is due to the

presence of free amine groups on the surface, which partially counteract the negative charge contributed by the silanol groups. Similarly, FSNPs with thiourea linkages obtained by reaction of isothiocyanated dye molecules with APS possess even lower colloidal stability and precipitate in ethanol and water at $\text{pH} \geq 7$.

Adducts **5** and **6** are synthesized from **8** instead of APS. Thus, FSNPs fabricated from these compounds are anticipated to show high surface charges. This is indeed the case. As shown in **Figure 8**, FSNP-1 and FSNP-3 exhibit reasonably high zeta potentials even at pH 3. With an increase in the pH value or the solution basicity, their potentials become higher or more negative because the dissociation of the surface silanol groups is favorable in such media.

2.6. Cell Imaging

One of the important areas in which FSNPs have demonstrated great potential is in cancer cell imaging. The AIE luminogens are benign to the growth of living cells.^[33] They are also nontoxic to HeLa cells and interfere little with the

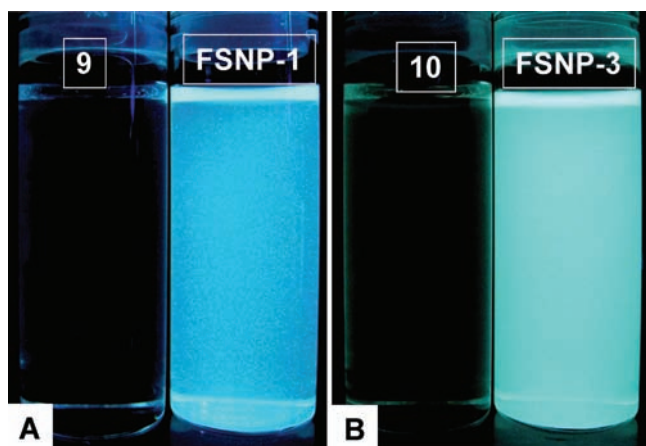


Figure 6. Photographs of ethanol solutions of A) **9** and FSNP-1 and B) **10** and FSNP-3 taken under the illumination of a UV lamp at 365 nm.

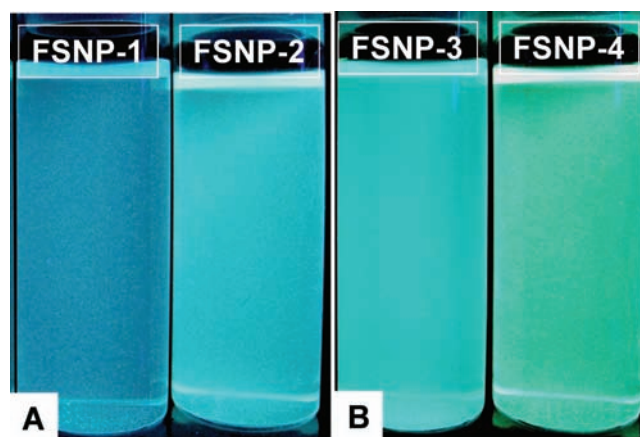


Figure 7. Photographs of ethanol solutions of A) FSNP-1 and FSNP-2 and B) FSNP-3 and FSNP-4 taken under the illumination of a UV lamp at 365 nm.

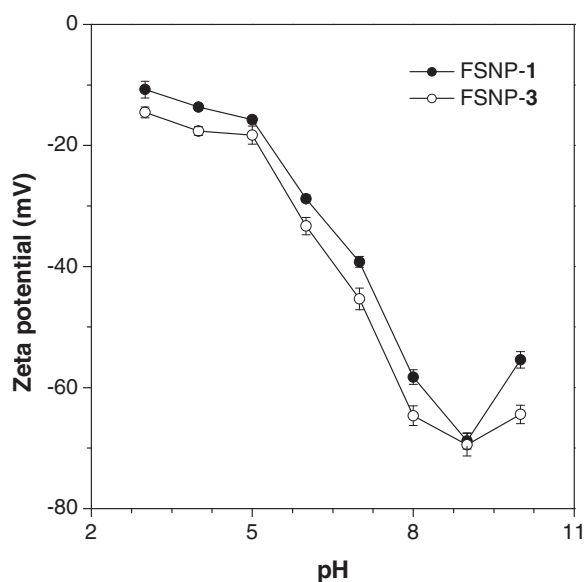


Figure 8. Zeta potentials of FSNP-1 and FSNP-3 at different pH values.

cytoplasmic activities of the cells. To examine the cell staining ability of our FSNPs, we cultured HeLa cells in the presence of these nanoparticles. After 6 h of incubation, the FSNPs are endocytosed through the cell membrane and efficiently anchor on the cytoplasmic organelles. To compare the uptake efficiency of FSNPs with different sizes, we stained the cells with FSNP-1 and FSNP-2. As depicted in **Figure 9**, both FSNPs work as good fluorescent visualizers for intracellular imaging. On the contrary, the images of HeLa cells stained by FSNP-3 and FSNP-4 show different brightness, albeit to a small extent (**Figure 10**).

During the endocytosis, the FSNPs are enclosed by the cell membrane to form small vesicles, which are then internalized in the cytoplasmic compartment of the cell. The FSNPs are further processed in the endosomes and lysosomes containing numerous digestive enzymes and are eventually released to the cytoplasm.^[34–36] When bound to the biomacromolecules, the FSNPs may emit even more intensely because their

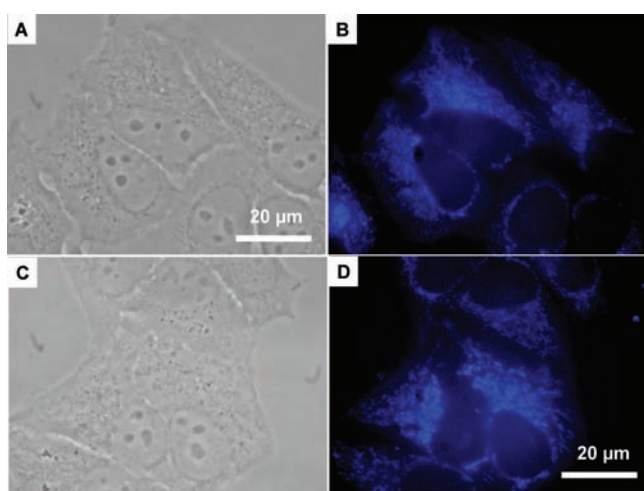


Figure 9. A,C) Bright-field and B,D) fluorescence images of HeLa cells labeled with A,B) FSNP-1 and C,D) FSNP-2.

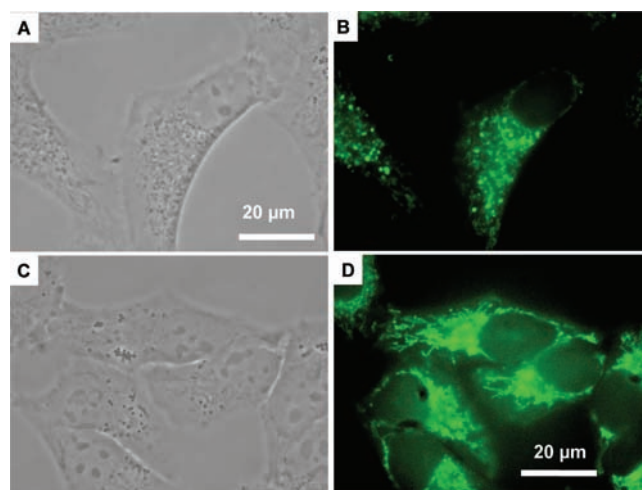


Figure 10. A,C) Bright-field and B,D) fluorescence images of HeLa cells labeled with A,B) FSNP-3 and C,D) FSNP-4.

intramolecular rotations are further restricted if some of them are located on the surface. Although the silica shells are hydrophilic, no fluorescence is observed in the cell nucleus, probably due to the “large” particle sizes of the FSNPs.

3. Conclusion

TPE- and silole-functionalized siloxanes have been facilely prepared by Cu(I)-catalyzed alkyne–azide 1,3-dipolar cycloaddition, and their one-pot, two-step sol–gel reaction with TEOS furnished FSNPs with uniform sizes and smooth surfaces. The sizes of the FSNPs are tunable by varying the fabrication method. Upon photoexcitation, the FSNPs emit strong blue and green light in high fluorescence quantum yields. They possess high surface charges and hence exhibit excellent colloidal stability. The FSNPs are benign to living cells and function as fluorescent visualizers for intracellular imaging of HeLa cells. Such attributes make the nanoparticles promising for an array of biological applications. Because of the rich acetylene chemistry, we are currently working on the incorporation of AIE luminogens with different emission colors into the silica network using the same strategy. Thanks to the high functionality tolerance of the click reaction, the surface of the FSNPs can be conjugated with biomolecules for specific cancer cell labeling. Details will be published in due course.

4. Experimental Section

Materials: Tetraethoxysilane (TEOS), 3-chloropropyltriethoxysilane (7), DMF, THF, and other reagents were purchased from Aldrich and used as received. Dienes **9** and **10** were prepared according to our previous publications.^[31,32]

Instrumentation: ¹H and ¹³C NMR spectra were recorded on a Bruker ARX 400 spectrometer with tetramethylsilane (TMS; $\delta = 0$) as internal standard. HR mass spectra were recorded on a Finnigan TSQ 7000 triple quadrupole spectrometer operating in the MALDI–TOF mode. The morphologies of the FSNPs were investigated using

JOEL 2010 TEM and JOEL 6700F SEM instruments at an accelerating voltage of 200 and 5 kV. Their sizes were measured using TEM software (Digital micrograph 365 Demo), which gave values with two digits after the decimal point. Samples were prepared by drop-casting dilute dispersions of the FSNPs onto copper 400-mesh carrier grids covered with carbon-coated Formvar films. The solvent was evaporated at room temperature in open air. Fluorescence spectra were recorded on a Perkin–Elmer LS 50B spectrofluorometer with xenon discharge lamp excitation. Zeta potentials and particle sizes of the FSNPs were determined at room temperature by a Zeta Plus Potential Analyzer (Brookhaven Instruments Corporation, USA). In these experiments, the silica nanoparticles were dispersed in ultrapure water (18 M Ω cm). Therefore, the ionic strength was constant for each experiment. The pH of the suspension was controlled by adding 0.1 M ammonium hydroxide and 0.1 M hydrochloric acid.

Synthesis of 3-Azidopropyltriethoxysilane (8): 3-Chloropropyltriethoxysilane (5.0 mL, 20.85 mmol), sodium azide (5 g, 77 mmol), and dry DMF (50 mL) were added to a 100-mL two-necked round-bottomed flask. The solution was heated to 90 °C under a nitrogen atmosphere for 5 h. The low-boiling compounds were removed by distillation under reduced pressure (ca. 10 mm Hg), after which diethyl ether (100 mL) was added to the mixture. The precipitates were removed by filtration and the solvent was removed under vacuum. Distillation of the residual oil under reduced pressure (2 mm Hg) at 96 °C gave the desired product as a colorless liquid (3.3 g, 68%). ¹H NMR (400 MHz, CDCl₃), δ = 3.81 (q, 6H), 3.24 (t, 2H), 1.66–1.70 (m, 2H), 1.21 (t, 9H), 0.66 ppm (t, 2H); ¹³C NMR (100 MHz, CDCl₃), δ = 58.4, 53.8, 22.6, 18.2, 7.5 ppm; IR: 2977, 2927, 2883, 2734, 2098, 1284, 1165, 1084, 960, 779 cm⁻¹.

Click Reaction: Cycloaddition reactions of **8** with **9** and **10** were carried under nitrogen using Schlenk tubes. Typical experimental procedures for the synthesis of **5** and **6** are given below.

Compound **8** (20.0 mg, 0.081 mmol), **9** (15.4 mg, 0.0405 mmol), and Cu(PPh₃)₃Br (4.5 mg, 6 mol%) were placed in a 15 mL Schlenk tube. THF (2 mL) was then injected into the solution. After stirring at 60 °C for 24 h, the reaction mixture was diluted with THF (3 mL) and centrifuged at 3000 rpm for 15 min. During the reaction, water was carefully excluded to avoid the possible hydrolysis of **8**. The supernatant was decanted and concentrated. The adduct (**5**) was characterized by HR mass spectrometry.

Adduct **6** was synthesized by similar procedures using **8** (20.0 mg, 0.081 mmol), **10** (18.74 mg, 0.0405 mmol), and Cu(PPh₃)₃Br (4.5 mg, 6 mol%) in THF (2 mL).

Preparation of FSNP-1 and FSNP-3 by the Stöber Method: FSNP-**1** was prepared from **5** and TEOS by a two-step sol–gel reaction. Compound **5** (\approx 15 μ mol) was added to a mixture of ethanol (32 mL), ammonium hydroxide (0.64 mL), and distilled water (3.9 mL). The solution was stirred at room temperature for 30 min, after which an ethanol solution (5 mL) of TEOS (1 mL) was added dropwise. The solution was stirred at room temperature for an additional 24 h to coat the luminogenic nanocores with silica shells.^[37] After incubation, the mixture was centrifuged and the nanoparticles of FSNP-**1** were redispersed in ethanol under sonication for 5 min. The process was repeated three times and the FSNPs were dispersed in water or ethanol for further experiments. Similarly, sol–gel reaction of **6** with TEOS following the same procedure furnished FSNP-**3**.

Preparation of FSNP-2 and FSNP-4 by the Microemulsion Method: FSNP-**2** and FSNP-**4** were prepared according to the literature method.^[38] Typical procedures for the fabrication of FSNP-**2**

are given below. In a typical synthesis, micelles were prepared at room temperature by sonication of a homogeneous mixture of cyclohexane (30 mL), Triton X-100 (7.2 mL), *n*-heptanol (5.6 mL), and water (600 μ L) for 30 min. Ammonia solution (800 μ L, 28%) was then added. After magnetically stirring for 15 min, **5** (100 μ L) was injected. The solution was stirred for another 15 min. After dropwise addition of TEOS (400 μ L), the reaction mixture was stirred for 24 h at room temperature. The microemulsion was terminated by adding ethanol and the nanoparticles were isolated by centrifugation and washed with ethanol and water to remove the surfactant. The nanoparticles were then dried in a vacuum at room temperature.

Cell Culture: HeLa cells were cultured in minimum essential medium containing 10% fetal bovine serum and antibiotics (100 units mL⁻¹ penicillin and 100 μ g mL⁻¹ streptomycin) in a 5% CO₂ humidity incubator at 37 °C.

Cell Imaging: HeLa cells were grown overnight on a plasma-treated 25-mm round cover slip mounted onto a 35-mm petri dish with an observation window. The living cells were stained with FSNPs (200 μ L) and incubated for 6 h. The cells were imaged under an inverted fluorescence microscope (Nikon Eclipse TE2000-U); excitation = 330–380 nm, dichroic mirror = 400 nm. The images of the cells were captured using a digital CCD camera.

Supporting Information

Supporting Information is available from the Wiley Online Library or from the author.

Acknowledgements

We thank the Research Grants Council (603509, 601608, CUHK2/CRF/08, and HKUST2/CRF/10), the Innovation and Technology Commission (ITP/008/09NP and ITS/168/09), the University Grants Committee of Hong Kong (AoE/P-03/08), and the National Science Foundation of China (20974028).

This Full Paper is part of the Special Issue on Nanotechnology with Soft Matter.

- [1] H. Ow, D. R. Larson, M. Srivastava, B. A. Baird, W. W. Webb, U. Wiesner, *Nano Lett.* **2005**, *5*, 113.
- [2] L. Huang, S. Dolai, K. Raja, M. Kruk, *Langmuir* **2010**, *4*, 2688.
- [3] R. P. Bagwe, L. R. Hilliard, W. Tan, *Langmuir* **2006**, *9*, 4357.
- [4] S. Kim, T. Y. Ohulchanskyy, H. E. Pudavar, R. K. Pandey, P. N. Prasad, *J. Am. Chem. Soc.* **2007**, *129*, 2669.
- [5] T. Y. Ohulchanskyy, I. Roy, L. N. Goswami, Y. Chen, E. J. Bergey, R. K. Pandey, A. R. Oseroff, P. N. Prasad, *Nano Lett.* **2007**, *7*, 2835.
- [6] R. Kumar, I. Roy, T. Y. Ohulchanskyy, L. A. Vathy, E. J. Bergey, M. Sajjad, P. N. Prasad, *ACS Nano* **2010**, *4*, 699.
- [7] M. Yasuhiro, K. Kazunori, *Cancer Sci.* **2009**, *100*, 572.
- [8] A. M. Derfus, W. C. W. Chan, S. N. Bhatia, *Nano Lett.* **2004**, *4*, 11.
- [9] J. Yao, D. Larson, H. Vishwasrao, W. Zipfel, W. Webb, *Proc. Natl. Acad. Sci. USA* **2005**, *102*, 14284.
- [10] T. Pellegrino, S. Kudera, T. Liedl, A. Javier, L. Manna, W. Parak, *Small* **2005**, *1*, 48.

- [11] M. E. Akeman, W. C. W. Chan, P. Laakkonen, S. N. Bhatia, E. Ruoslahti, *Proc. Natl. Acad. Sci. USA* **2002**, *20*, 12617.
- [12] A. Burns, H. Ow, U. Wiesner, *Chem. Soc. Rev.* **2006**, *35*, 1028.
- [13] a) L. Wang, W. Zhao, W. Tan, *Nano Res.* **2008**, *1*, 99; b) S. Liu, Z. Tang, *J. Mater. Chem.* **2010**, *20*, 24.
- [14] S. Santra, K. Wang, R. Tapeç, W. Tan, *J. Biomed. Opt.* **2001**, *6*, 160.
- [15] M. Nakamura, M. Shono, K. Ishimura, *Anal. Chem.* **2007**, *79*, 6507.
- [16] J. B. Birks, *Photophysics of Aromatic Molecules*, Wiley, New York **1970**.
- [17] Z. Zhao, S. Chen, X. Shen, F. Mahtab, Y. Yu, P. Lu, J. W. Y. Lam, H. S. Kwok, B. Z. Tang, *Chem. Commun.* **2010**, 686.
- [18] Y. Hong, Y. Dong, H. Tong, M. Haeußler, J. W. Y. Lam, B. Z. Tang, *Polym. Prepr.* **2007**, *48*, 367.
- [19] H. Tong, Y. Dong, Y. Hong, M. Haeußler, J. W. Y. Lam, H. H. Y. Sung, X. Yu, J. Sun, I. D. Williams, H. S. Kwok, B. Z. Tang, *J. Phys. Chem. C* **2007**, *111*, 2287.
- [20] Y. Hong, J. W. Y. Lam, B. Z. Tang, *Chem. Commun.* **2009**, 4332.
- [21] J. Chen, B. Xu, X. Ouyang, B. Z. Tang, Y. Cao, *J. Phys. Chem. A* **2004**, *108*, 7522.
- [22] Z. Zhao, S. Chen, J. W. Y. Lam, P. Lu, Y. Zhong, K. S. Wong, H. S. Kwok, B. Z. Tang, *Chem. Commun.* **2010**, 2221.
- [23] Y. Hong, M. Haeußler, J. W. Y. Lam, Z. Li, K. Sin, Y. Q. Dong, H. Tong, J. Liu, A. Qin, R. Renneberg, B. Z. Tang, *Chem. Eur. J.* **2008**, *14*, 6428.
- [24] W. Z. Yuan, L. Ping, C. Shuming, J. W. Y. Lam, Z. Wang, L. Yang, H. S. Kwok, M. Yuguang, B. Z. Tang, *Adv. Mater.* **2010**, *22*, 2159.
- [25] H. Tong, Y. Hong, Y. Dong, M. Haeußler, J. W. Y. Lam, Z. Li, Z. F. Guo, Z. H. Guo, B. Z. Tang, *Chem. Commun.* **2006**, 3705.
- [26] R. Huisgen, *1,3-Dipolar Cycloaddition Chemistry* (Ed.: A. Padwa), Wiley, New York, **1984**, pp.1–176.
- [27] a) T. Lummerstorfer, H. Hoffmann, *J. Phys. Chem. B* **2004**, *108*, 3963; b) M. Slater, M. Snauko, F. Svec, J. M. Frechet, *J. Anal. Chem.* **2006**, *78*, 4969; c) V. V. Rostovtsev, L. G. Green, V. V. Fokin, K. B. Sharpless, *Angew. Chem. Int. Ed.* **2002**, *41*, 2596; d) C. W. Tornøe, C. Christensen, M. Meldal, *J. Org. Chem.* **2002**, *67*, 3057; e) H. C. Kolb, M. G. Finn, K. B. Sharpless, *Angew. Chem. Int. Ed.* **2001**, *40*, 2004.
- [28] A. V. Blaaderen, J. V. Geest, A. Vrij, *J. Colloid Interface Sci.* **1992**, *154*, 481.
- [29] J. H. Zhang, P. Zhan, Z. L. Wang, W. Y. Zhang, N. B. Ming, *J. Mater. Res.* **2003**, *18*, 649.
- [30] K. S. Rao, K. El-Hami, T. Kodaki, K. Matsushige, K. Makino, *J. Colloid Interface Sci.* **2005**, *289*, 125.
- [31] P. Lu, J. W. Y. Lam, J. Liu, C. K. W. Jim, W. Yuan, N. Xie, Y. Zhong, Q. Hu, K. S. Wong, K. K. L. Cheuk, B. A. Tang, *Macromol. Rapid Commun.* **2010**, *31*, 834.
- [32] J. Liu, Y. Zhong, J. W. Y. Lam, P. Lu, Y. Hong, Y. Yu, Y. Y. Yue, F. Mahtab, H. H.-Y. Sung, I. Williams, K. S. Wong, B. Z. Tang, *Macromolecules* **2010**, *43*, 4921.
- [33] F. Mahtab, Y. Hong, J. Liu, Y. Yu, J. W. Y. Lam, A. Qin, P. Lu, B. Z. Tang, *Chem. Eur. J.* **2010**, *16*, 4266.
- [34] S. D. Conner, S. L. Schmid, *Nature* **2003**, *422*, 37.
- [35] M. Marsh, H. T. McMahon, *Science* **1999**, *285*, 215.
- [36] M. Breunig, S. Bauer, A. Goepferich, *Eur. J. Pharm. Biopharm.* **2008**, *68*, 112.
- [37] W. Stöber, A. Fink, J. Bohn, *J. Colloid Interface Sci.* **1968**, *26*, 62.
- [38] R. P. Bagwe, C. Yang, L. R. Hilliard, W. Tan, *Langmuir* **2004**, *20*, 8336.

Received: December 6, 2010
 Revised: January 17, 2011
 Published online: April 26, 2011